Published in final edited form as:
Nat Neurosci. 2016 August ; 19(8): 999–1002. doi:10.1038/nn.4331.

Glucose responsive neurons of the paraventricular thalamus control sucrose-seeking behavior

Gwenaël Labouèbe[1], **Benjamin Boutrel**[2], **David Tarussio**[1], and **Bernard Thorens**[1]

[1]Center for Integrative Genomics, University of Lausanne, Lausanne Switzerland [2]Center for Psychiatric Neuroscience, Lausanne University Hospital, Lausanne, Switzerland

Abstract

Feeding behavior is governed by homeostatic needs and motivational drive to obtain palatable foods. Here, we identify a population of glutamatergic neurons in the paraventricular thalamus, which express the glucose transporter Glut2 (*Scl2a2*) and project to the nucleus accumbens. These neurons are activated by hypoglycemia and, in freely moving mice, their activation by optogenetics or *Slc2a2* inactivation increases motivated sucrose but not saccharin-seeking behavior. These neurons may control sugar overconsumption in obesity and diabetes.

The brain depends almost exclusively on glucose as a source of metabolic energy. Sufficient provision of glucose to the brain is ensured by homeostatic mechanisms, which maintain glycemia at a minimal level of ~ 5 mM 1 and by hedonic mechanisms, which attribute a high reward value to glucose-containing foods to increase the motivation to consume them 2, 3. In this hedonic response the nucleus accumbens plays a central regulatory role by integrating feeding-related inputs originating from several brain areas 4–11.

In previous studies, we showed that Glut2 expression in the nervous system (NG2KO mice) is required for the control by glucose of the sympathetic and parasympathetic nerve activities 12. Here, we tested whether neuronal Glut2-dependent glucose-sensing was also involved in motivated feeding behavior. NG2KO mice and control littermates were monitored during operant conditioning tasks, which associate nose poking behavior with a light stimulus (conditioned stimulus, CS+) and the delivery of a sweet reward (10% sucrose solution). In a first set of experiments, mice were trained for 30 minutes daily for 10 days on a fixed ratio 1 schedule of reinforcement (FR1) where they learned to associate the CS+ with sweet reward. Appetitive learning was observed in both genotypes since reward obtained and active nosepokes performed increased over time (Fig. 1a,b) whereas inactive nosepokes

Correspondence: Bernard Thorens, Center for Integrative Genomics, Genopode Building, University of Lausanne, CH-1015 Lausanne Switzerland. Phone: +41 21 692 3981, Fax: +41 21 692 3985, Bernard.Thorens@unil.ch.

Author Contributions: BT, GL, BB designed the experimental strategy and analyzed the data. DT performed histological analysis and supervised mouse breeding. All other experiments were performed by GL. BT and GL wrote the manuscript. All authors commented on the manuscript.

Competing financial interests: The authors declare no competing financial interests.

Europe PMC Funders Author Manuscripts

remained similarly low in NG2KO mice and control mice (Suppl. Fig. 1a) indicating similar learning capacity. However, NG2KO mice performed better in this task (Fig. 1a,b). Next, we subjected mice to a progressive ratio (PR) schedule, which consisted of a systematic within-session increase in the number of nosepokes required to earn each successive reward. NG2KO mice again performed better, with higher number of active nosepokes, of rewards obtained, and a higher maximal operant response (breakpoint) indicating higher motivation (Fig. 1c-e). Similar behavioral tasks were then performed with the non-caloric artificial sweetener saccharin. In FR1 (Fig. 1f,g) and PR (Fig. 1h-j) experiments NG2KO mice and control mice performed identically indicating that neuronal Glut2-dependent glucose sensing responds to sucrose and is insensitive to artificial sweeteners.

Operant conditioning is associated with activity of the nucleus accumbens (NAc) 13, 14. We therefore investigated whether Glut2-positive neurons or axons could be observed in the NAc using *Slc2a2-cre;Rosa26tdtomato* mice 15. We observed numerous red fibers within the medial part of the NAc, mainly close to the anterior commissure and around the ventral end of the lateral ventricle (Suppl. Fig. 2a). To determine the origin of those fibers, we performed retrograde tracing experiments in which the cholera toxin B subunit-AlexaFluor 488 conjugate (CTxB) was injected bilaterally in the NAc of *Slc2a2-cre;Rosa26tdtomato* mice (Fig. 2a and Suppl. Fig. 2b). Three weeks later, we screened the entire brain for tdtomato cell bodies labeled with CTxB. No colabeling with the rare Glut2-neurons present in the ventral tegmental area, the prefrontal cortex, the hippocampus or the different hypothalamic nuclei could be found. Co-labeled cells were found only in the paraventricular thalamic nucleus (PVT) (Fig. 2b) where 91 ± 1.7% of the PVT Glut2 neurons were also labeled with CTxB.

Next, we assessed whether the firing activity of tdtomato positive neurons was responsive to changes in extracellular glucose concentrations (Fig. 2c). In the presence of 5 mM glucose these neurons showed a low basal activity, which was markedly enhanced in the presence of 0.5 mM glucose. Returning the glucose to 5 mM restored the initial firing activity (Fig. 2d-f). The same glucose-dependent increase in firing activity was seen in the presence a cocktail of synaptic inhibitors indicating that glucose-sensing is cell-autonomous (Suppl. Fig. 3a). When glycolysis was inhibited by 10 mM glucosamine in the presence of 5 mM glucose, firing was significantly increased (Fig. 2g-i). Fructose at 5 mM failed to suppress firing induced by 0.5 mM glucose (Suppl. Fig. 3b). Finally, patch clamp analysis of Glut2 neurons from mice previously injected with 2-deoxy-D-glucose showed that their firing frequency at 5 mM glucose was identical to that seen during exposure to 0.5 mM glucose of Glut2-neurons from naïve mice and did not change when glucose was lowered to 0.5 mM (Fig. 2j-l). Tdtomato negative cells were also recorded in the presence of 5 or 0.5 mM glucose; they were found to be unresponsive to hypoglycemia (Suppl. Fig. 3c). Thus, PVT Glut2 neurons are activated by low glucose concentrations or by glycolysis inhibition; their firing rate cannot be suppressed by fructose, and they are responsive to *in vivo* induced neuroglucopenia.

To investigate the nature of Glut2 projections to the NAc, *Slc2a2-cre* mice were injected in the PVT with an AAV-DIO-ChR2-eYFP 16 (Fig. 3a). Brain slices obtained three weeks later displayed numerous eYFP-positive neurons in the PVT and fibers in the NAc (Fig. 3b,c).

Electrophysiological recordings from medium spiny neurons (MSNs) of the NAc together with local light-stimulation of the ChR2-expressing terminals (Fig. 3c) revealed postsynaptic inward currents (Fig. 3d), which could be totally abolished by tetrodotoxin, a blocker of action potential-dependent neurotransmitter release (Fig. 3d,e). The typical fast kinetics of those inward currents suggested they were α-amino-3-hydroxy-5-methyl-4-isoxazolepropionic receptors (AMPARs) excitatory post-synaptic currents (EPSCs). This was confirmed by the application of the AMPAR antagonist DNQX that entirely suppressed light-induced EPSCs in all the cells tested (Fig. 3f-g). Thus, light-stimulation of NAc-projecting PVT Glut2-neurons triggers glutamate release onto NAc MSNs.

To test the functional role of the PVT Glut2 excitatory inputs onto the NAc, we used an operant conditioning protocol associated with *in vivo* optogenetic activation of these neurons. *Slc2a2-cre* mice and control mice were injected in the PVT with an AAV-DIO-ChR2-eYFP and equipped with a fiber-optic cannula. Following recovery, mice were tested during operant conditioning to obtain sucrose. At the beginning of each behavioral session, mice were connected to a light source via an optical fiber and stimulated during the entire duration of the session. During the training/learning period (FR1 schedule), the ChR2-expressing mice consumed significantly more reward (Fig. 3h) and performed more active nosepokes (Fig. 3i) than the control mice. Moreover, during the progressive ratio schedule mice expressing ChR2 showed increased motivated sucrose-seeking behavior by obtaining more rewards and showing increased breakpoint (Fig. 3j,k). To confirm that increased motivated behavior was light-dependent we tested the same mice in a progressive ratio schedule one month later without light stimulation. No difference in motivated behavior was seen between genotypes (Suppl. Fig. 4b,c). A similar experiment was repeated but with light stimulation through fiber-optic cannulas placed bilaterally at the NAc level. Light stimulation increased motivated sucrose seeking behavior as assessed in FR1 and progressive ratio schedules (Suppl. Fig. 5). When tested three days later without light stimulation, the breakpoint value of control mice remained the same and ChR2-expressing mice exhibited similar motivation as controls. Note that learning during the FR1 protocol was slower as compared to the previous experiment (Fig 3h,i), probably because these mice were implanted with two (instead of one) optical fibers, which may hamper access to the nosepoke holes.

Finally, we inactivated *Slc2a2* selectively in the PVT of $Slc2a2^{loxP/loxP}$ mice by stereotactic injection of an AAV-Cre-GFP (Fig 3l). PCR analysis of genomic DNA extracted from the PVT and fluorescence microscopy analysis confirmed proper injection of the virus and recombination of $Slc2a2^{floxed}$ allele in the AAV-Cre-GFP injected mice (Suppl. Fig. 6). These mice displayed increased motivation to get sucrose compared to control mice as reflected by the higher number of rewards and increased breakpoint (Fig. 3m,n).

Collectively, our data show that Glut2-neurons from the PVT and projecting to the NAc form a population of hypoglycemia-activated, glutamatergic neurons, which induce EPSCs in MSN neurons. Their firing rate can be increased by glycolysis inhibition, but cannot be suppressed by fructose, indicating that they are controlled by glucose metabolism. When activated by hypoglycemia, optogenetics, or by *Slc2a2* inactivation, they increase motivated sugar-feeding behavior indicating a dominant role in motivated sugar seeking. The possible

relevance of these results to human physiology is suggested by the observations that mild hypoglycemia induces marked increase in synaptic activity in this part of the thalamus 17 and that variants in *SLC2A2* are associated with increased intake of sugar-containing foods 18 and conversion from impaired glucose tolerance to type 2 diabetes 19. This newly identified neuronal pathway may, thus, represent a new target for the prevention of metabolic disease aiming at restoring the normal balance between the homeostatic and hedonic control of food intake.

Online Methods

Mice

All procedures were approved by the veterinary office of Canton de Vaud (Switzerland) under the veterinary license number VD2513. *Slc2a2*$^{loxP/loxP}$, *Slc2a2*$^{\Delta/loxP}$;*Nes*$^{Cre/+}$ (NG2KO), *Slc2a2-cre* and *Slc2a2-cre;Rosa26tdtomato* mice were as described previously20–22. NG2KO and *Slc2a2*$^{loxP/loxP}$ mice were on a mixed C57BL/6;SV129 background; *Slc2a2-cre* and *Glut2-cre;Rosa26tdtomato* mice were on a C57BL/6 background. All studies used littermates as controls. For all experiments, mice were age-matched and randomly assigned to experimental groups to ensure a non-biased animals distribution. No blinding was used. Unless otherwise stated, animals were collectively housed (maximum 5 individuals per cage) on a 12-hour light/dark cycle (lights on at 7 am) and fed with a standard chow (Diet 3436, Provimi Kliba AG).

Viral vectors

All viral constructs were produced by the Vector Core of the Gene Therapy Center at the University of North Carolina (UNC, North Carolina, USA).

Operant conditioning

Adult NG2KO males and control littermates (10 to 15 weeks old) were housed individually under a 12-h reversed light/dark cycle (lights on at 8:30 pm) at a constant temperature (22 ± 1°C) and had ad libitum access to water. Starting from the first day of experiment, mice were slightly food restricted and received ~3 g of laboratory chow per day. No more than 15 % of body weight reduction over the entire duration of the experiment was allowed. Mice were trained in operant conditioning chambers (Med Associates) under a fixed ratio 1 schedule of reinforcement (FR1) during 30-min daily sessions. Animals had choice between two nosepoke ports, an active nosepoke hole associated with a 3-sec light cue and a concomitant delivery of a liquid reward through a central spout equipped with infrared head entry detector and an inactive nosepoke hole that remained inoperative. Each active nosepoke triggered the delivery of 10 µl of a 10 % sucrose or 0.2 % saccharin solution. Liquid rewards remained available for 3 sec once access to the central spout was detected. Supplementary entries in the active nosepoke in the absence of head entry detection above the liquid dipper and entries in the inactive nosepoke were recorded but had no further consequence. After a training period of 7 to 10 days, the animals were engaged into three consecutive sessions (one 90 min session per day) under a progressive-ratio schedule of reinforcement (PR). Under this schedule the mice were required to progressively increase the number of active nosepokes between two successive rewards based on the progression

sequence given by23: response ratio (rounded to nearest integer) = $(5e^{(\text{reward}\times 0.2)}) - 5$. Hence, the progressive-ratio schedule followed the progression: 1, 2, 4, 6, 9, 12, 15, 20, 25, 32, 40, 50, 62, 77, 95, 118, 145, 178, 219, etc. The maximal number of active nosepokes performed to reach the final ratio was defined as the breakpoint, a value reflecting animals' motivation to get the reward. Active/inactive nosepokes and reward obtained were monitored online using an analog/digital interface coupling the operant chambers to a computer running the MED-PC behavioral software suite (Med Associates).

Neuronal retrograde tracing

Four adult *Slc2a2-cre;Rosa26tdtomato* males (10 weeks old) were anesthetized with isoflurane (5% (w/v) for induction followed by 2.5% for maintenance (Attane, Piramal Healthcare)) and placed in a stereotaxic frame (David Kopf Instruments). Nucleus accumbens (NAc) was infused bilaterally with cholera toxin subunit B (CTxB) conjugated with AlexaFluor 488 (Molecular Probes, Life Technologies). The following stereotaxic coordinates were used: AP +1.5 / ML ± 1.4 / DV -4,5 mm (10° angle). A volume of 0.4 µl of 0.25 % CTxB solution was injected in each hemisphere through 33 Gauge stainless steel injector (Hamilton) coupled to a precision pump (Harvard Apparatus) with a injection rate of 0.1 µl . min^{-1}. Two weeks later, animals were anesthetized (isoflurane) and perfused transcardially with a 0.1 M phosphate buffer (PBS, pH 7.4) followed by 4% paraformaldehyde in PBS. The perfused brains were dissected and postfixed with 4% paraformaldehyde in PBS at 4 °C for 1 h and then placed overnight at 4 °C in a solution containing 30% sucrose in PBS. Brains were frozen in isopentane and maintained at -20 °C until further analysis. Twenty-five micrometers cryosections were prepared (Leica) and mounted onto glass slides with Mowiol anti-fade medium (Sigma-Aldrich). Images were taken using an Axio Imager D1 microscope interfaced with a Axiovision software or a LSM 510 Meta inverted confocal laser scanning microscope with LSM software 3.5 (Zeiss). For neuronal quantification, four sections containing PVT were screened in each mouse (n = 4) and Glut2 neurons were counted (n = 891) to determine which percentage of those neurons were colabeled with CTxB. Injection sites were verified for each mouse at the end of the experiment.

Electrophysiology

4 to 8 weeks old males used for electrophysiology were deeply anesthetized with isoflurane prior to decapitation, brain removed and immediately submerged in a ice-cold slushy ACSF solution saturated with 95 % O_2 / 5 % CO_2 containing (in mM): 125 NaCl, 2.5 KCl, 1.25 NaH2PO4, 1 MgCl2, 2 CaCl2, 26 NaHCO3, 12.5 sucrose and 5 mM glucose (300 ± 5 mOsm). Acute coronal sections (250 µm) containing PVT or NAc were obtained using a vibratome (VT1000S; Leica) and maintained at 32°C for at least 1 h before recording. Experiments were performed using an upright epifluorescence microscope (BX51WI; Olympus) mounted on a motorized stage and coupled to micromanipulators (Sutter instruments). Brain slices were placed in a recording chamber and continuously superfused at a rate of 2 ml . min^{-1} with oxygenated ACSF maintained at 32 - 34 °C. Borosilicate pipettes (resistance = 3 to 5 MΩ; Harvard Apparatus) were shaped with a horizontal micropipette puller (Sutter Instruments). Firing rate of PVT neurons at different extracellular glucose concentrations (5 or 0.5 mM) was monitored after a 10-15 min baseline through

loose cell-attached recordings in current-clamp mode using a MultiClamp 700B amplifier (Molecular Devices). Intra-pipette solution contained (in mM): 130 potassium gluconate, 10 HEPES, 0.2 EGTA, 5 NaCl, 1 MgCl, 10 Na-phosphocreatinine, 4 MgATP and 0.5 Na_2GTP (pH 7.2-7.3, 275 ± 5 mOsm). When mentioned in the text, a cocktail of synaptic inhibitors was used and was composed of picrotoxin (100 μM; GABAA receptor antagonist), DNQX (10 μM; AMPA and kainate receptor antagonist), DL-AP5 (100 μM; NMDA receptor antagonist) and strychnine (1 μM; glycine receptor antagonist)(Tocris Bioscience). For *ex vivo* optogenetic experiments in medium spiny neurons of the NAc, neurons were voltage clamped at −70 mV in whole-cell configuration and light-induced currents were recorded with a intra-pipette solution containing (in mM): 117 cesium methanesulfonate, 20 HEPES, 0.4 EGTA, 2.8 NaCl, 5 TEA-Cl, 2.5 MgATP and 0.5 Na_2GTP (pH 7.2-7.3, 275 ± 5 mOsm). Blue light (473 nm) pulses were delivered on the brain slice through the microscope objective. TTX 1 μM and DNQX 10 μM were bath applied in the perfusion chamber. Currents traces were constructed by averaging 15 consecutive photocurrents. Signals were filtered at 2 kHz, digitized at 10 kHz and collected online using a pClamp 10 data acquisition system (Molecular Devices).

Optogenetics

10 to 12 weeks old adult *Slc2a2-cre* or *Slc2a2*$^{+/+}$ males were used for optogenetics experiments. Under isoflurane anesthesia mice were placed in a stereotaxic frame (David Kopf Instruments) and PVT was infused with the viral vector rAAV2-Ef1α- DIO-hChR2(H134R)-eYFP (titer = 3.08 x 10^{12} particles . ml^{-1}) to allow the expression of channelrhodopsin-2 in a Cre-dependent manner (0.25 μl delivered at 0.1 μl . min^{-1}). To ensure a good expression of the ChR2 in the entire PVT the virus was injected at two coordinates: AP -0.4 / ML +0.8 / DV -3.5 mm and AP -1.6 / ML +0.7 / DV -3 mm with a 10° angle to avoid the damage to the superior sagittal sinus. Three weeks after viral injection mice were either used for *ex vivo* electrophysiological experiments or involved in *in vivo* operant conditioning behavioral tasks as described above. For *ex vivo* experiments, 4 ms light pulses were delivered by a high-power collimated blue LED system (M470L2-C1 + LEDD1B; Thorlabs) through the optical path of the microscope. For *in vivo* experiments, optical fiber cannulas (Precision Fiber Products) were lowered either unilaterally in PVT (AP -0.4 / ML +0.8 / DV -3.4 mm, 10° angle) or bilaterally in NAc (AP +1.5 / ML ±1.35 / DV -4.2 mm, 10° angle) and fixed to the skull with surgical screws (PlasticsOne), tissue adhesive (VetBond; 3M) and dental cement (Paladur; Heraeus-Kulzer). A DSPP laser (LRS-0473-GFM-00100-05; Laserglow Technologies) was used to deliver light pulses (10 ms light pulses at 20 Hz, 1 s on/1s off, 10-15 mW) through an optical fiber (0.22 NA, 200 μm core diameter; Doric Lenses) that was attached to the optic cannula at the beginning of each experimental session (FR1 or PR). Light-stimulation was applied during the entire duration of the experimental session. To avoid the optical fiber from twisting and to allow mice to move freely, a rotary joint (FRJ 1×1; Doric Lenses) was placed outside the operant chamber right on top of the animal. Injection sites and optical fiber cannula placement were verified for each mouse at the end of the experiment.

PVT Glut2 deletion

10 to 15 weeks old adult *Slc2a2*$^{loxP/loxP}$ males were injected with the viral vectors rAAV5-Cre-GFP (titer = 5 x 10^{12} particles . ml^{-1}) or rAAV5-TRUFR-GFP (titer = 6.9 x 10^{12} particles . ml^{-1}) at the following injections sites: AP -0.4 / ML +0.8 / DV -3.5 mm (10° angle) and AP -1.6 / ML +0.7 / DV -3.0 mm (10° angle). Each injection consisted in an infusion of 0.25 µl virus at a speed of 0.1 µl . min^{-1}. At the end of the operant conditioning experiments, mice were anesthetized (isoflurane), sacrificed and deletion of Glut2 was determined via PCR amplification of genomic DNA from dissected brain tissue containing PVT as previously described24. PCR amplification gels were made in duplicates. Injection site was verified for each mouse at the end of the experiment.

Statistical analysis

Statistical significance was calculated using GraphPad Prism 5.0c (GraphPad Software). The sample size for each experiment was determined based on published studies using similar experimental design together with pilot experiments from our laboratory. This allowed us to determined the sample size required for each experiment to ensure a statistical power of 0.8 and an alpha level of 0.05. Two-sided Student's *t*-tests were used to analyze statistical significance between two experimental groups. To ensure variance similarity between compared groups, a Fischer's F-test was performed before each t-test. When multiple comparisons was required, one-way or two-way ANOVA was performed followed by a Bonferroni's post-hoc test. The data distribution was assumed to be normal. Data are represented as means ± s.e.m. The levels of statistical significance are indicated as follow: *** P<0.001 ; ** P<0.01 ; * P<0.05.

Data availability

Data are available upon request from the first author (Bernard.Thorens@unil.ch).

Supplementary Material

Refer to Web version on PubMed Central for supplementary material.

Acknowledgements

The authors would like to thank Pr. Christophe Magnan for help with preliminary feeding experiments. This work was supported by grants to BT from the Swiss National Science Foundation (3100A0B-128657) and a European Research Council advanced grant (INSIGHT).

References

1. Unger RH, Orci L. Glucagon and the A cells. Physiology and Pathophysiology. N Engl J Med. 1981; 304:1518–1524. [PubMed: 7015132]
2. Berridge KC, Robinson TE, Aldridge JW. Dissecting components of reward: 'liking', 'wanting', and learning. Curr Opin Pharmacol. 2009; 9:65–73. [PubMed: 19162544]
3. Volkow ND, Wang GJ, Tomasi D, Baler RD. The addictive dimensionality of obesity. Biological psychiatry. 2013; 73:811–818. [PubMed: 23374642]
4. Sclafani A, Ackroff K. Reinforcement value of sucrose measured by progressive ratio operant licking in the rat. Physiol Behav. 2003; 79:663–670. [PubMed: 12954407]

5. Levine AS, Kotz CM, Gosnell BA. Sugars: hedonic aspects, neuroregulation, and energy balance. Am J Clin Nutr. 2003; 78:834S–842S. [PubMed: 14522747]
6. Norgren R, Hajnal A, Mungarndee SS. Gustatory reward and the nucleus accumbens. Physiol Behav. 2006; 89:531–535. [PubMed: 16822531]
7. Sclafani A. Oral, post-oral and genetic interactions in sweet appetite. Physiol Behav. 2006; 89:525–530. [PubMed: 16647093]
8. Sclafani A. Sucrose motivation in sweet "sensitive" (C57BL/6J) and "subsensitive" (129P3/J) mice measured by progressive ratio licking. Physiol Behav. 2006; 87:734–744. [PubMed: 16530236]
9. Smith GP. Accumbens dopamine mediates the rewarding effect of orosensory stimulation by sucrose. Appetite. 2004; 43:11–13. [PubMed: 15262012]
10. Hajnal A, Smith GP, Norgren R. Oral sucrose stimulation increases accumbens dopamine in the rat. Am J Physiol Regul Integr Comp Physiol. 2004; 286:R31–37. [PubMed: 12933362]
11. Salamone JD, Correa M. The mysterious motivational functions of mesolimbic dopamine. Neuron. 2012; 76:470–485. [PubMed: 23141060]
12. Tarussio D, et al. Nervous glucose sensing regulates postnatal beta cell proliferation and glucose homeostasis. J Clin Invest. 2014; 124:413–424. [PubMed: 24334455]
13. Gale JT, Shields DC, Ishizawa Y, Eskandar EN. Reward and reinforcement activity in the nucleus accumbens during learning. Frontiers in behavioral neuroscience. 2014; 8:114. [PubMed: 24765069]
14. Corbit LH, Balleine BW. The general and outcome-specific forms of Pavlovian-instrumental transfer are differentially mediated by the nucleus accumbens core and shell. J Neurosci. 2011; 31:11786–11794. [PubMed: 21849539]
15. Lamy CM, et al. Hypoglycemia-Activated GLUT2 Neurons of the Nucleus Tractus Solitarius Stimulate Vagal Activity and Glucagon Secretion. Cell Metab. 2014; 19:527–538. [PubMed: 24606905]
16. Mounien L, et al. Glut2-dependent glucose-sensing controls thermoregulation by enhancing the leptin sensitivity of NPY and POMC neurons. Faseb J. 2010; 24:1747–1758. [PubMed: 20097878]
17. Arbelaez AM, et al. Thalamic activation during slightly subphysiological glycemia in humans. Diabetes Care. 2012; 35:2570–2574. [PubMed: 22891254]
18. Eny KM, Wolever TM, Fontaine-Bisson B, El-Sohemy A. Genetic variant in the glucose transporter type 2 is associated with higher intakes of sugars in two distinct populations. Physiol Genomics. 2008; 33:355–360. [PubMed: 18349384]
19. Laukkanen O, et al. Polymorphisms in the SLC2A2 (GLUT2) gene are associated with the conversion from impaired glucose tolerance to type 2 diabetes: the Finnish Diabetes Prevention Study. Diabetes. 2005; 54:2256–2260. [PubMed: 15983230]
20. Mounien L, et al. Glut2-dependent glucose-sensing controls thermoregulation by enhancing the leptin sensitivity of NPY and POMC neurons. Faseb J. 2010; 24:1747–1758. [PubMed: 20097878]
21. Tarussio D, et al. Nervous glucose sensing regulates postnatal beta cell proliferation and glucose homeostasis. J Clin Invest. 2014; 124:413–424. [PubMed: 24334455]
22. Lamy CM, et al. Hypoglycemia-Activated GLUT2 Neurons of the Nucleus Tractus Solitarius Stimulate Vagal Activity and Glucagon Secretion. Cell Metab. 2014; 19:527–538. [PubMed: 24606905]
23. Richardson NR, Roberts DC. Progressive ratio schedules in drug self-administration studies in rats: a method to evaluate reinforcing efficacy. J Neurosci Methods. 1996; 66:1–11. [PubMed: 8794935]
24. Seyer P, et al. Hepatic glucose sensing is required to preserve beta cell glucose competence. J Clin Invest. 2013; 123:1662–1676. [PubMed: 23549084]

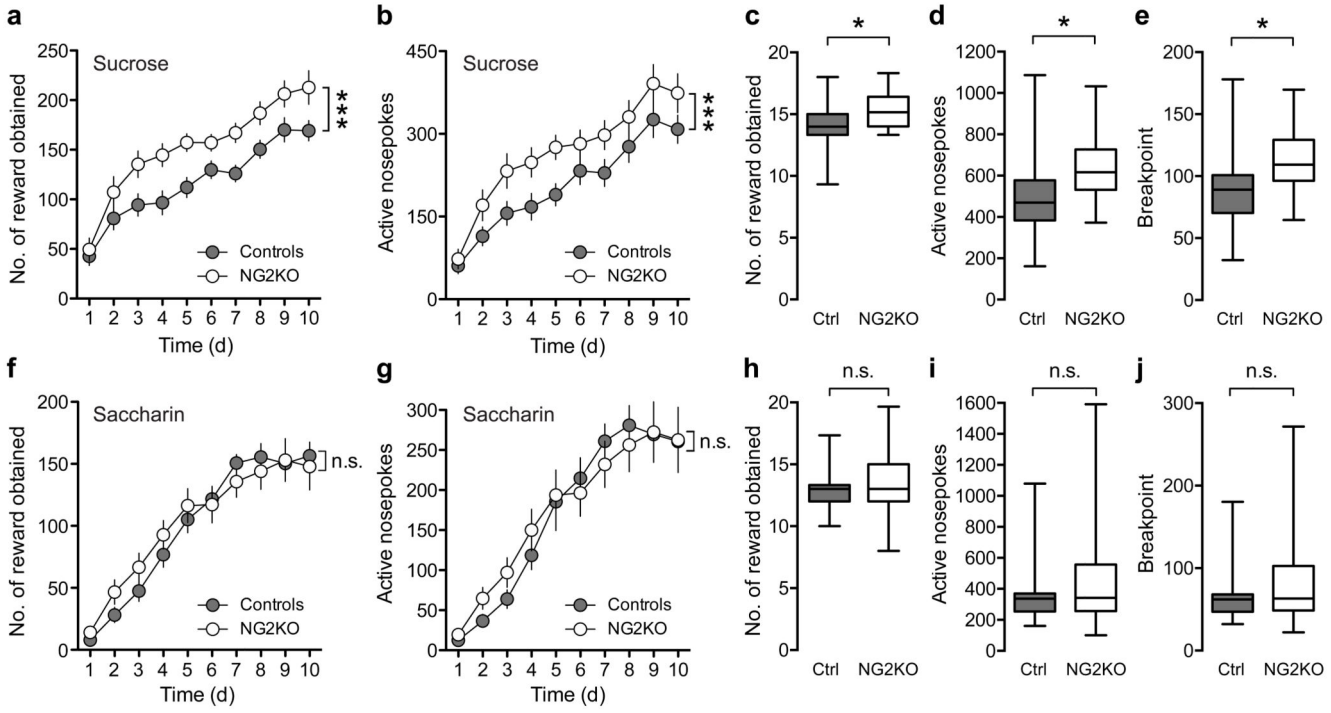

Figure 1. Inactivation of *Slc2a2* enhances motivated sucrose-seeking behavior.

In operant conditioning experiments, under fixed ratio schedule (FR1), NG2KO mice (n=18) showed higher performance to obtain a sucrose reward as compared to control mice (n=22). **a**, Rewards obtained (30-min daily session). **b**, Active nosepokes (Reward: genotype effect, $F(1,341) = 47.29$, $P<0.0001$; interaction, $F(9,341) = 0.65$, $P = 0.7574$; Active nosepokes: genotype effect, $F(1,341) = 29.07$, $P<0.0001$; interaction, $F(9,341) = 0.38$, $P = 0.9449$; two-way ANOVA followed by Bonferroni's test). Under progressive ratio (PR) schedule, NG2KO mice showed higher motivation to obtain sucrose as shown by **c**, the total number of rewards ($P = 0.0314$), **d,** the number of active nosepokes ($P = 0.0320$), and **e**, the breakpoint ($P = 0.03$; t-test). With saccharin as reward (0.2% solution) NG2KO (n=17) and control (n= 19) littermates behaved identically in FR1 (**f**, **g**) (Reward: genotype effect, $F(1,335) = 0.47$, $P = 0.4915$; interaction, $F(9,335) = 0.67$, $P = 0.7403$; Active nosepokes: genotype effect, $F(1,335) = 0.14$, $P = 0.7111$; interaction, $F(9,335) = 0.42$, $P = 0.9235$; two-way ANOVA followed by Bonferroni's test), or PR (**h-j**) schedule, ($P>0.05$, t-test). Graphs show means ± s.e.m; boxplots show median, lower and upper quartiles (box), and minimum and maximum (whiskers). *** $P<0.001$; * $P<0.05$; n.s.: non significant.

Europe PMC Funders Author Manuscripts

Europe PMC Funders Author Manuscripts

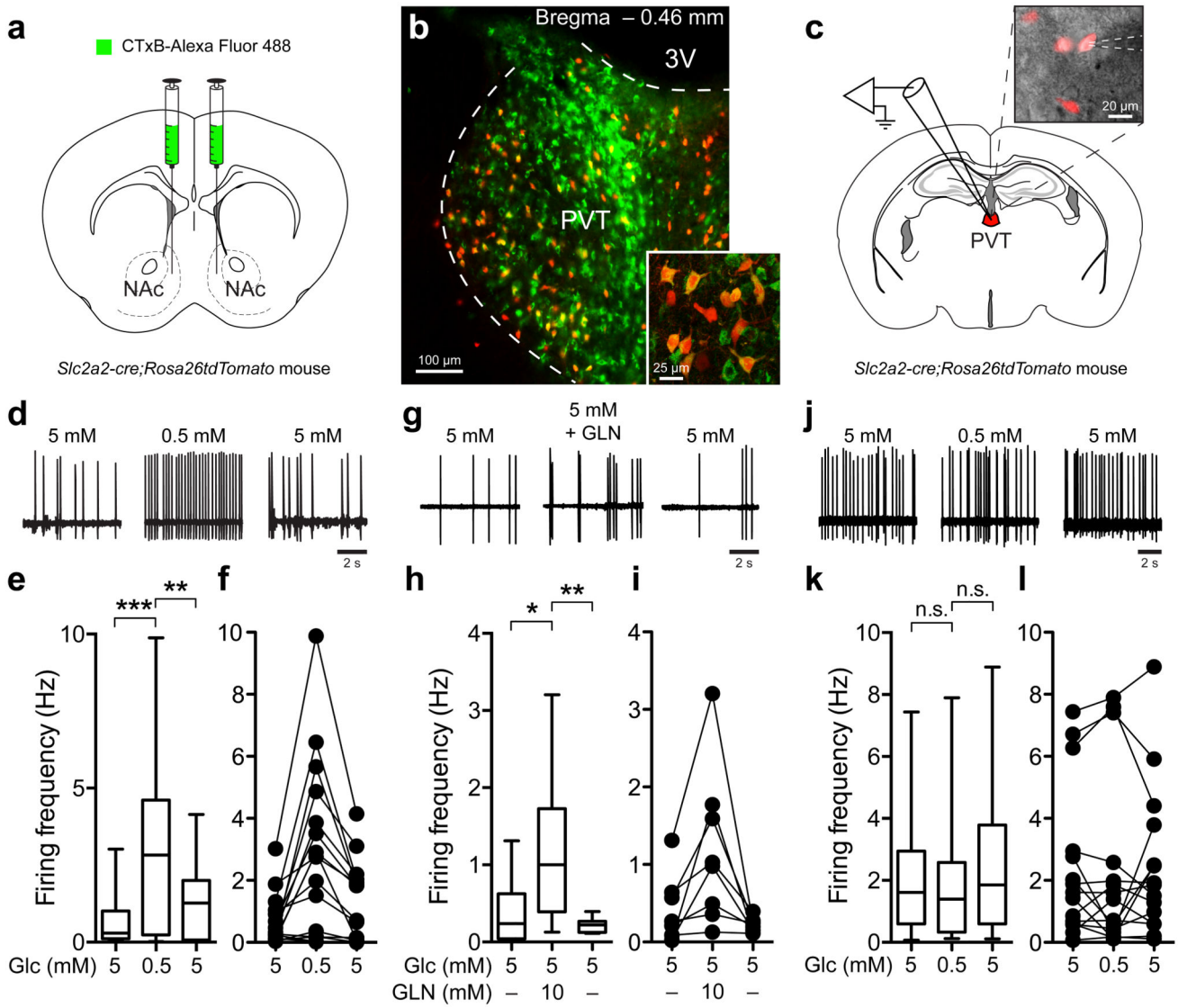

Figure 2. PVT Glut2 neurons project to NAc and respond to hypoglycemia.

a, Schematic of the experimental approach. CTxB was bilaterally injected in the NAc of *Slc2a2-cre*;*Rosa26tdtomato* mice. **b**, CTxB (green) was found to co-localize with tdtomato-positive Glut2 neurons (red) only in the PVT area. **c**, *Slc2a2-cre;Rosa26tdtomato* mice were used to prepare acute brain slices containing the PVT Glut2 neurons for patch-clamp analysis. Inset shows microscopic view of a patched Glut2 neuron (red); white dashed lines delimit the recording pipette. **d**, Neuronal activity recorded in cell-attached configuration from a PVT Glut2 neuron in the presence of the indicated extracellular glucose concentrations. **e**, Mean firing frequency monitored under the different extracellular glucose (Glc) concentrations (n = 16 neurons in 7 mice). Hypoglycemia induced a significant increase of the firing rate ($F(2,15) = 14.49$, $P<0.0001$; one-way ANOVA followed by a Bonferroni's test). **f**, Individual plots of firing frequency for the neurons described in panel **e**. **g**,**h**, D-glucosamine (GLN) induced an increase of the Glut2 neuronal activity despite the presence of 5 mM extracellular glucose (n = 8 neurons in 4 mice; $F(2,7) = 7.9$, $P = 0.0051$;

one-way ANOVA followed by a Bonferroni's test). **i**, Individual plots for neurons described in panel **h**. **j**, Neuroglucopenia induced by i.p. 2-DG 45 min prior to sacrifice increased neuronal activity of PVT Glut2 neurons. **k**, Mean firing frequency monitored under the indicated extracellular glucose concentrations (n = 15 neurons in 8 mice). Injection of 2-DG increased the firing activity in the presence of 5 mM glucose and blunted the response to hypoglycemia (compare with **e**) ($F(2,14) = 0.11$, $P = 0.8976$; one-way ANOVA followed by a Bonferroni's test). **l**, Individual plots for neurons described in panel **k**. Boxplots show median, lower and upper quartiles (box), and minimum and maximum (whiskers). Nucleus accumbens (NAc), paraventricular thalamic nucleus (PVT) and third ventricule (3V). : *** $P<0.001$; ** $P<0.01$; * $P<0.05$; n.s.: non significant.

Europe PMC Funders Author Manuscripts

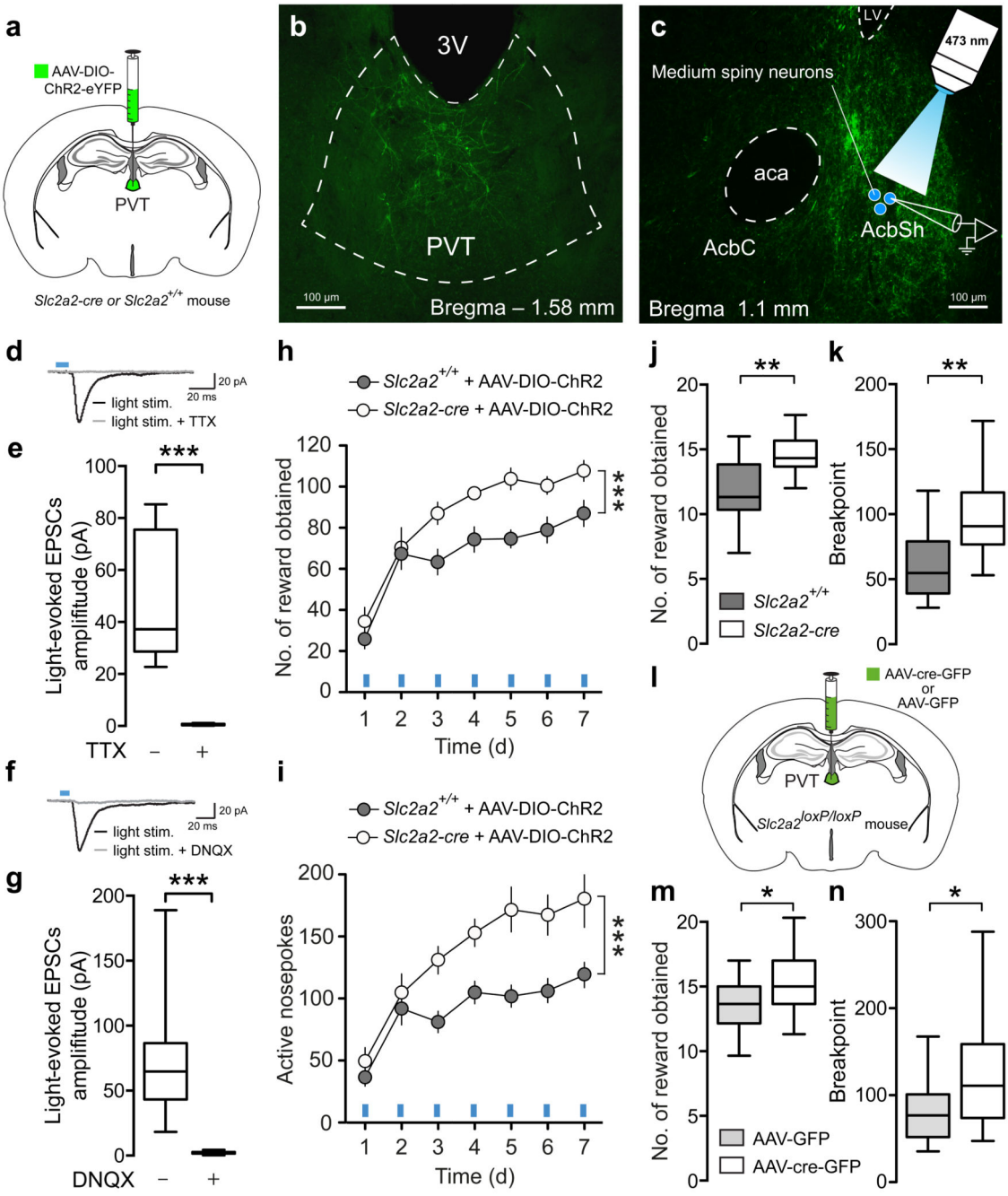

Figure 3. PVT Glut2 neurons are glutamatergic and control motivated sucrose-seeking behavior.

a, Schematic of the experimental approach. ChR2 was virally delivered in PVT of *Slc2a2-cre* or control mice (*Slc2a2*$^{+/+}$). **b**, Epifluorescence microscopy picture of ChR2-positive neurons (green fluorescence, YFP) in the PVT of a *Slc2a2-cre* mouse. **c**, Schematic of the experimental protocol. NAc medium spiny neurons (blue circles) were recorded while distal axons of PVT Glut2 neurons (green fluorescence) were photostimulated in the NAc of a *Slc2a2-cre* mouse transfected with ChR2 in the PVT. **d**, Example of light-induced currents obtained during baseline condition (black trace) or in the presence of tetrodotoxin (TTX, 1

Europe PMC Funders Author Manuscripts

µM, grey trace). Blue rectangles indicate light pulse (4 ms, 473 nm). **e**, Mean amplitude of light-induced currents recorded in NAc medium spiny neurons in baseline condition or with TTX (n = 7, P = 0.0002, paired t-test). **f**, Example of light-induced currents obtained during baseline condition (black trace) or in the presence of the AMPAR antagonist DNQX (10 µM, grey trace). **g**, Similar to **e** with DNQX instead of TTX (n = 13, P<0.0001, paired t-test). **h**,**i**, FR1 operant conditioning for sucrose coupled with *in vivo* light stimulation of Glut2 PVT neurons in control (grey circles, n = 13) or *Slc2a2-cre* mice (white circles, n = 15) which received prior PVT injection of AAV-DIO-ChR2. Blue rectangles indicate light pulses (473 nm, 10 ms light pulses at 20 Hz, 1 s on/1s off). Light-evoked neuronal activation increased operant responses to obtain sucrose (Reward: genotype effect, $F(1,182) = 32.79$, $P<0.0001$; interaction, $F(6,182) = 1.16$, $P = 0.3282$; Active nosepokes: genotype effect, $F(1,182) = 38.57$, $P<0.0001$; interaction, $F(6,182) = 1.49$, $P = 0.1830$; two-way ANOVA followed by Bonferroni's test). **j**, Mean sucrose reward and **k**, breakpoint value monitored under progressive ratio schedule with *in vivo* light stimulation of Glut2 PVT neurons in control (grey boxes) or *Slc2a2-cre* mice (white boxes)(P = 0.0011 and P = 0.0042, respectively; t-test). **l**, Schematic view of the experimental approach. AAV-Cre-GFP or the control construct AAV-GFP was injected in PVT of $Slc2a2^{loxP/loxP}$ mice (n = 17 and n = 18 respectively). **m**, Mean sucrose reward and **n**, breakpoint value monitored under progressive ratio schedule in $Slc2a2^{loxP/loxP}$ injected with AAV-GFP (grey boxes) or AAV-Cre-GFP (white boxes)(P = 0.0347 and P = 0.0213, respectively; *t*-test). Graphs show means ± s.e.m; Boxplots show median, lower and upper quartiles (box), and minimum and maximum (whiskers). Nucleus accumbens core (AcbC), shell (AcbSh), lateral ventricule (LV) and anterior commissure (aca). *** P<0.001 ; ** P<0.01 ; * P<0.05.